

# A high temperature superconducting demonstrator coil for ARCOS: a novel toroidal magnetic spectrometer for an astroparticle physics experiment in space

Magnus Dam,<sup>a,\*</sup> William Jerome Burger,<sup>b,c</sup> Rita Carpentiero,<sup>d</sup> Enrico Chesta,<sup>e</sup> Roberto Iuppa,<sup>f</sup> Gijs de Rijk<sup>e</sup> and Lucio Rossi<sup>a,g</sup>

<sup>a</sup>INFN, National Institute for Nuclear Physics  
I-20133 Milano MI, Italy

<sup>b</sup>CREAF, Enrico Fermi Research Center  
I-00184 Roma RM, Italy

<sup>c</sup>TIFPA, Trento Institute for Fundamental Physics and Applications,  
I-38122 Trento TN, Italy

<sup>d</sup>ASI, Italian Space Agency,  
I-00133 Rome RM, Italy

<sup>e</sup>CERN, European Organization for Nuclear Research,  
CH-1211 Geneva 23, Switzerland

<sup>f</sup>University of Trento, Department of Physics,  
I-38122 Trento TN, Italy

<sup>g</sup>University of Milan, Department of Physics,  
I-20133 Milano MI, Italy

E-mail: [magnus.dam@mi.infn.it](mailto:magnus.dam@mi.infn.it)

A magnetic spectrometer determines the signed rigidity of charged particles by measuring their trajectories in the presence of a magnetic field. High Temperature Superconducting (HTS) magnets can operate in space without the use of a cryogenic liquid. While HTS magnets have many potential applications in space, including active magnetic radiation shielding, we present the design of an HTS magnetic spectrometer with a toroidal magnet providing a bending strength of 3 T m. The toroidal magnet is about 2 m in outer diameter, 2 m in height, and requires about 60 km of 12 mm wide ReBCO HTS tape. The magnet operates with an engineering current density of 855 A/mm<sup>2</sup> at a temperature of 20 K and a peak magnetic flux density of about 12 T. In the context of the HTS Demonstrator Magnet for Space (HDMS) project, we have designed and are building a small-scale coil pack of the toroidal magnet. The demonstrator magnet consists of two racetrack-like coils enclosed with copper bands that function as current leads and layer jumps. The no-insulation winding method facilitates self-protection against quenches. A lightweight mechanical structure made from aluminum alloy supports the coils.

37<sup>th</sup> International Cosmic Ray Conference (ICRC 2021)  
July 12th – 23rd, 2021  
Online – Berlin, Germany

---

\*Presenter

## 1. Introduction

High Temperature Superconducting (HTS) magnets can operate in space without the need for a liquid cryogen. They have many potential applications in space including radiation shielding [1, 2], but the most accessible application is arguably for a next generation magnetic spectrometer.

The Alpha Magnetic Spectrometer (AMS-02) [3] is the state-of-the-art experiment searching for antimatter in cosmic rays [4]. It is based on a permanent magnet providing a central magnetic flux density of  $B_c = 0.15$  T. AMS-02 was installed in May 2011 as an external module of the International Space Station and it is the largest magnetic spectrometer ever operated in space. The AMS-02 results have increased our knowledge of antimatter in cosmic rays in multiple ways: (i) The so-called positron excess [5] hinted by the PAMELA and Fermi-LAT collaborations has been carefully characterized up to 1 TeV, (ii) the antiproton flux [6] has been measured up to 0.45 TeV, (iii) AMS-02 has detected about one antihelium-3 or antihelium-4 candidate events per year during the last 10 years (energies below 100 GeV) [7], a measurement that suggests new physics beyond the standard model of cosmic rays. The future contributions from AMS-02 are expected to be incremental considering that the Maximum Detectable Rigidity (MDR) is 2 TV for  $|Z| = 1$  particles [8] for a geometrical acceptance of  $0.3 \text{ m}^2\text{sr}$ . The possibility to confirm the existence of antinuclei with energies larger than tens of GeV, as well as the measurement of the antiproton flux up to 100 TeV, motivate the need for a next generation magnetic spectrometer in space.

AMS-100 [9] is a proposed next generation magnetic spectrometer for space, based on a large thin-walled HTS solenoid generating a central magnetic flux density of  $B_c = 1$  T. ALADINO [10] is another proposal for a magnetic spectrometer based on a 10-coil toroidal HTS magnet providing an average bending strength of 1.1 T m.

This paper presents ARCOS (Astroparticle Research Compact Orbital Spectrometer), a compact magnetic spectrometer operating in space with an acceptance of  $2.8 \text{ m}^2\text{sr}$  and MDR of 50 TV for protons and antiprotons. ARCOS is based on a high-field toroidal HTS magnet providing an average bending strength of 3 T m. A toroidal magnet was chosen to naturally obtain a zero magnetic moment, while a solenoid as proposed for AMS-100 on the contrary requires a compensation coil to balance the magnetic moment. The ARCOS magnet is smaller and with a much higher magnetic field than the toroidal magnet proposed for ALADINO. ARCOS relies on the development of a high-field HTS magnet system suitable for long-term operation in space. An HTS demonstrator coil for the ARCOS magnet is being built within the HTS Demonstrator Magnet for Space (HDMS) project [11].

## 2. Astroparticle Research Compact Orbital Spectrometer (ARCOS)

We require ARCOS to have a MDR of 50 TV for protons and antiprotons. Assuming a maximum resolution of the detectors of  $5 \mu\text{m}$ , this necessitates a bending strength of 3 T m. A compact design makes the launch possible with cost-effective commercial launchers. The geometric acceptance of the spectrometer is  $2.8 \text{ m}^2\text{sr}$  for protons and antiprotons. Launching several identical spectrometers over a few years would further increase the acceptance, significantly lowering risks and costs compared to launching a single large spectrometer.

## 2.1 The toroidal magnet system

The ARCOS magnet is a toroidal HTS magnet composed of 12 racetrack-shaped double-pancake coils, and it provides the 3 Tm bending strength of the spectrometer. A toroidal magnet has inherently a vanishing magnetic moment which is necessary to avoid uncontrolled rotations caused by interplanetary magnetic fields. The magnet operates at 20 K to enable cooling without a cryogenic liquid. The magnet will instead be cooled by a combination of a sun-shield and an electrically powered cryocooler. The coils are wound from 12 mm wide commercial HTS tape. The winding turns are non-insulated to make the magnet self-protected against quenches. To provide self-regulated current sharing between winding turns we consider to use a metal-insulator transition (MIT) [12] material such as vanadium (III) oxide ( $V_2O_3$ ). We consider mechanically stabilizing the winding block against vibrations by adding solder [13] or electrically conductive epoxy resin [14] between winding turns. Mechanical design will follow the criteria used in Ref. [1] for a space toroid envisioned for magnetic shielding.

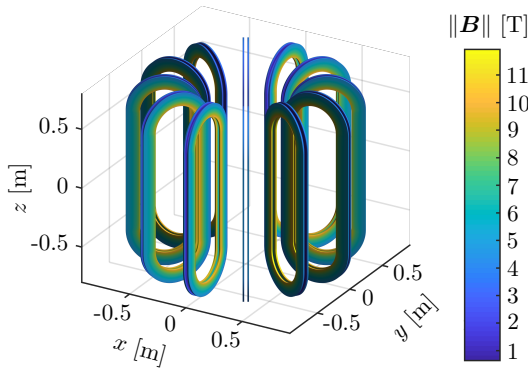


**Figure 1:** The magnetic flux density  $B$  on the surface of the ARCOS magnet that consists of 12 racetrack-shaped double-pancake coils.

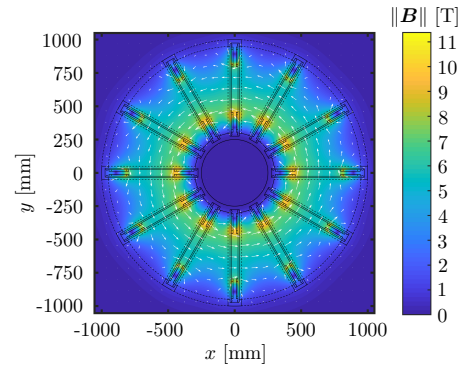


**Figure 2:** The magnetic flux density  $B$  in the cross sectional plane overlaid with the contours of the mechanical structure.

Figure 1 shows the magnetic flux density  $B$  on the surface of the toroidal coils. The engineering operating current density of the winding blocks is  $J_e = 855 \text{ A/mm}^2$  with a peak magnetic flux density on the conductor of  $B_{\text{peak}} = 11.9 \text{ T}$ . Figure 2 shows the magnetic flux density  $B$  in the central cross-sectional plane of the toroid and the contours of the mechanical structure. The mechanical structure is made from aluminum 2050-T84. The ARCOS magnet is still in the conceptual design stage, and a more detailed design will be produced after basic design choices has been tested with demonstrator coils.

## 2.2 Detector system

Figure 3 shows the toroidal magnet with the baseline detector systems: a tracker, composed of silicon pixel detectors, which measure the charged particle trajectories in the magnetic field, and plastic scintillators, which provide the trigger to select the desired event topologies. The silicon pixel detector tracker planes are located concentrically around the toroidal axis. The outermost planes measure the direction of the incident particle as it enters or exits the magnetic field. Multiple measurements of the track position are recorded along the particle trajectory. The plastic scintillator planes consist of two segmented cylinders located concentrically around the toroidal axis.

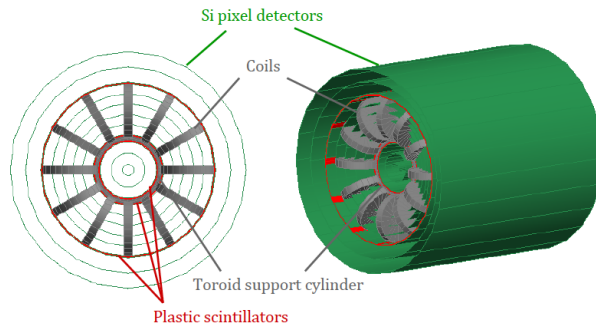


**Figure 3:** On the left: a cross-sectional view of the silicon pixel detector planes (green), plastic scintillator planes (red), toroidal coils and cylindrical support structure (gray). On the right: A three-dimensional view.

### 2.3 Particle simulations

Figures 4 and 5 illustrates Geant4 [15] simulation results of event topologies for 10 GV protons (p) and electrons ( $e^-$ ) passing through ARCOS. The p in Fig. 4 enters the magnetic field between the coils, passes through the support cylinder and disappears in an inelastic nuclear interaction in the other side of the support cylinder. The  $e^-$  in Fig. 5 follows the same initial trajectory, however in the presence of the magnetic field, colinear synchrotron radiation (SR) is generated.

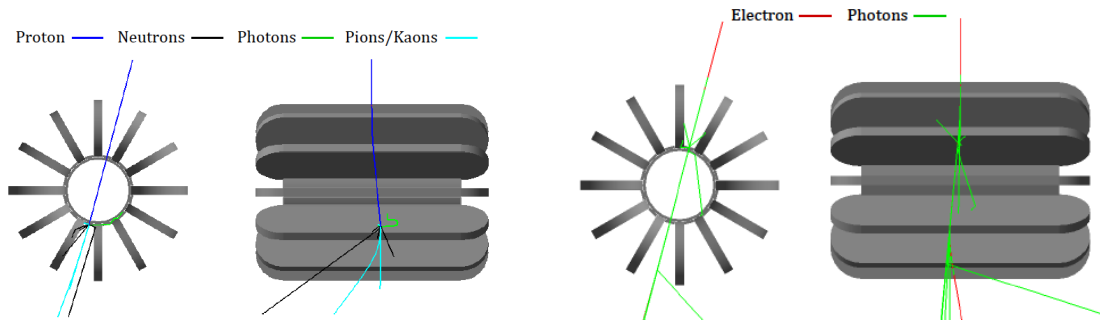


**Figure 4:** 10 GV proton Geant4 simulation event. The detectors shown in Fig. 3 are present in the simulation, but not shown in the event display.

**Figure 5:** 10 GV electron Geant4 simulation event. The detectors shown in Fig. 3 are present in the simulation, but not shown in the event display.

A preliminary study based on an 8-coil toroid was made to estimate spectrometer performance for protons and positrons in terms of the MDR and corresponding acceptances. The track positions were recorded in the Outer, Middle and Inner plastic scintillator planes which define the acceptance, and provide the information to calculate the deflection in the magnetic field used to estimate the MDR. The deflection is along the axis of the toroid for the acceptance defined by the trigger planes as illustrated in Figs. 6 and 7. Only the support cylinder and wire-frame views of the trigger planes are displayed. The p entering the magnetic field region at the top of Fig. 6 deflects in the  $-\hat{z}$ -direction, traverses the field-free region inside the support cylinder, and deflects in the  $+\hat{z}$ -direction on the exit side at the bottom of the figure. The  $z$ -deflection observed between the trigger planes defining the entry side, cylinder, and exit side regions, is proportional to the rigidity. The deflection of the  $e^-$  in Fig. 7 is in the opposite direction of the p in Fig. 6, and shifted with respect to the SR photons on the exit side.

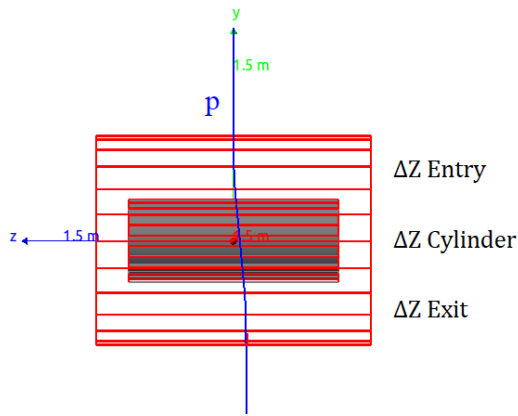


**Figure 6:** The deflection along the axis of the toroid of a 10 GV proton in the magnetic field.

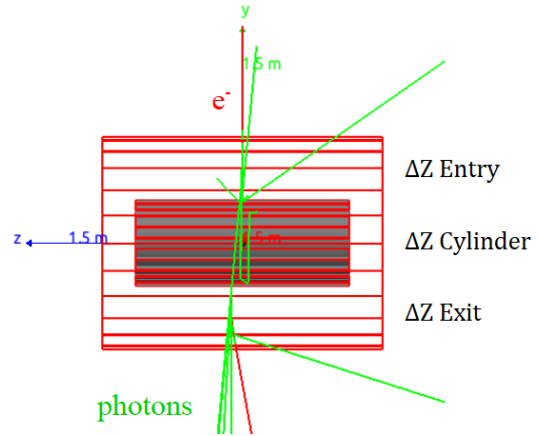


**Figure 7:** The deflection along the axis of the toroid of a 10 GV electron in the magnetic field.

The acceptance was computed by generating 500k particles uniformly distributed on the four lateral surfaces parallel to the toroidal axis of a  $3 \times 3 \times 3 \text{ m}^3$  cube surrounding the spectrometer. The p rigidity acceptance and the corresponding deflection observed along the  $\hat{z}$ -direction across the entry side field region ( $\Delta Z1$ ) are presented in Fig. 8. The trigger acceptances refer to the Outer, Middle and Inner trigger planes on the entry (O1, M1, I1) and exit (I2, M2, O2) sides of the spectrometer defined by the direction of the incident p. The p acceptances are constant above 10 GV at about 3.65, 2.75 and 0.15  $\text{m}^2\text{sr}$  for all, O1-M1-I1 (+) and pass-through trigger plane combinations. The values of  $\Delta Z1$  are 1, 2.5, 5 and 20  $\mu\text{m}$  respectively at 250, 100, 50 and 10 TV. The p MDR, where the measurement error is 100%, is about 50 TV for an estimated position resolution of 5  $\mu\text{m}$  for the tracker. About 15% of the protons interact with the 5 cm thick aluminum support cylinder.

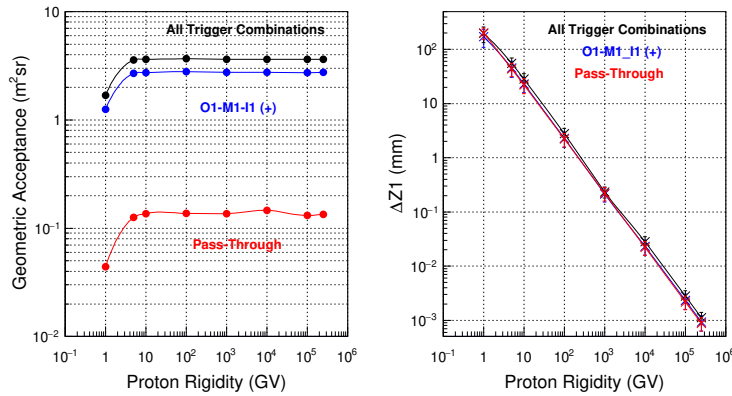


**Figure 8:** Left: Proton rigidity acceptance. Right: The corresponding deflection  $\Delta Z1$  across the entry side field region. The quoted errors represent the RMS variation of the average value of the  $\Delta Z1$  distributions.

The positron ( $e^+$ ) acceptance and deflection are shown in Fig. 9. The differences observed with the p results in Fig. 8 are explained by the radiation losses of the high energy positrons due to bremsstrahlung in the material of the magnet structure, and SR in the magnetic field. The ultrarelativistic positrons lose on average about 50% of their initial energy in the 5 cm thick aluminum support cylinder due to bremsstrahlung. The fractional energy lost in SR is 0.80, 0.20

and 0.025 for 100, 10 and 1 TeV positrons. The radiation losses explain the rigidity dependence of the  $e^+$  acceptance. The average deflection across the entry side field region ( $\Delta Z1$ ) are comparable to the  $p$  values between 1 and 10 GV, although the root-mean-square (RMS) variation of the  $e^+$  distributions are larger. Above 10 GV both the average and RMS values increase with respect to the  $p$  values in Fig. 8. The average (RMS) values of the positron  $\Delta Z1$  are 0.050 (0.070), 0.280 (0.380), 2.85 (4.00) and 5.95 (5.40) mm respectively at 100, 10, 1 and 0.1 TV. The SR loss dominate the deflection measurement error.

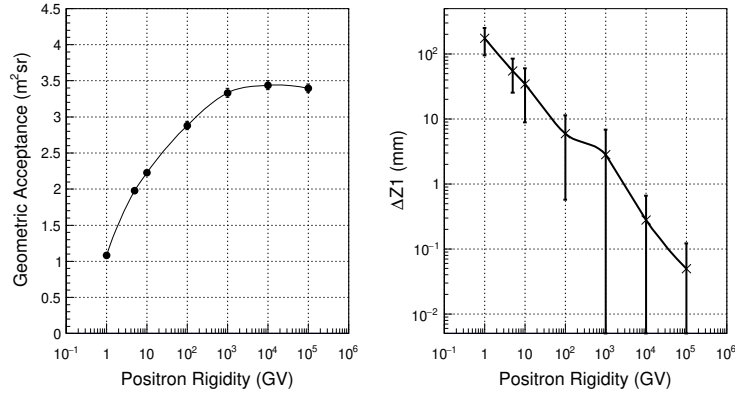


**Figure 9:** Left: Positron rigidity acceptance. Right: The corresponding deflection  $\Delta Z1$  across the entry side field region. The quoted errors represent the RMS variation of the average value of the  $\Delta Z1$  distributions.

### 3. HTS demonstrator magnet for space

The HTS Demonstrator Magnet for Space (HDMS) project [11] aims to design, build and test an HTS demonstrator coil for the ARCOS magnet. Three coil versions of the AMaSED (Advanced Magnetic Spectrometer Experimental Demonstrator) are planned to be manufactured: AMaSED-0 is a mechanical model coil without superconducting material, AMaSED-1 is an electrical model containing a single coil using medium performance HTS tape, while AMaSED-2 is the final demonstrator coil with two pancake layers containing high-performance HTS tape.

#### 3.1 AMaSED-2 coil design

AMaSED-2 is a small-scale demonstrator magnet for a single coil pack of the ARCOS magnet. The AMaSED-2 coils will be wound from two co-wound 12 mm SuperPower HTS tapes. Figure 10 shows the critical current  $I_c$  of the two-tape-stack cable as function of the magnetic flux density  $B$  for different temperatures together with the loadline for AMaSED-2.

Figure 11 shows the theoretical maximum magnetic flux density  $B$  on the surface of AMaSED-2 operating at the 4.2 K critical current,  $I_{op} = 2480 \text{ A/mm}^2$ . The winding block has an outer diameter of 256 mm and a height of 480 mm. The shape is racetrack-like, with the straight segments of the racetrack shape replaced by circular arcs to make it easier to obtain a tight winding. The total winding block thickness is 28 mm corresponding to about 144 winding turns. On the inside and on the outside of each winding block are copper bands to mechanically support the shape of the winding block and transport the current into and out from the HTS tape with a large contact surface for a small contact resistance.

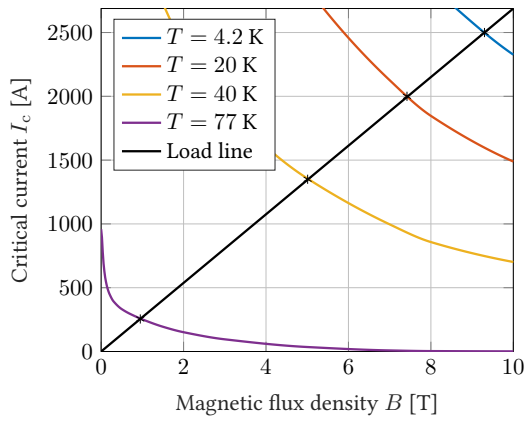


**Figure 10:** The critical current  $I_c$  as function of the magnetic flux density  $B$  for different temperatures for a two-tape-stack SuperPower cable together with the loadline for AMaSED-2.

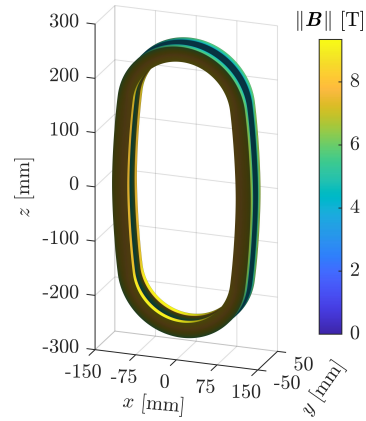


**Figure 11:** The theoretical maximum magnetic flux density on the surface of AMaSED-2 at 4.2 K. The peak magnetic flux density is 9.3 T.

### 3.2 Mechanical structure

The mechanical structure consists of a magnet former that is a thick aluminum plate with the shapes of the coils machined into. Insulation shells are inserted into the former, whereafter the coils are inserted. The coils are covered with insulation shells and closed off with cover plates. A copper interconnection block transfers the current between coil layers. Figure 12 shows an exploded view of AMaSED-0. AMaSED-2 uses aluminum 2050-T84 instead of aluminum 6082-T64, otherwise the design is mostly the same.

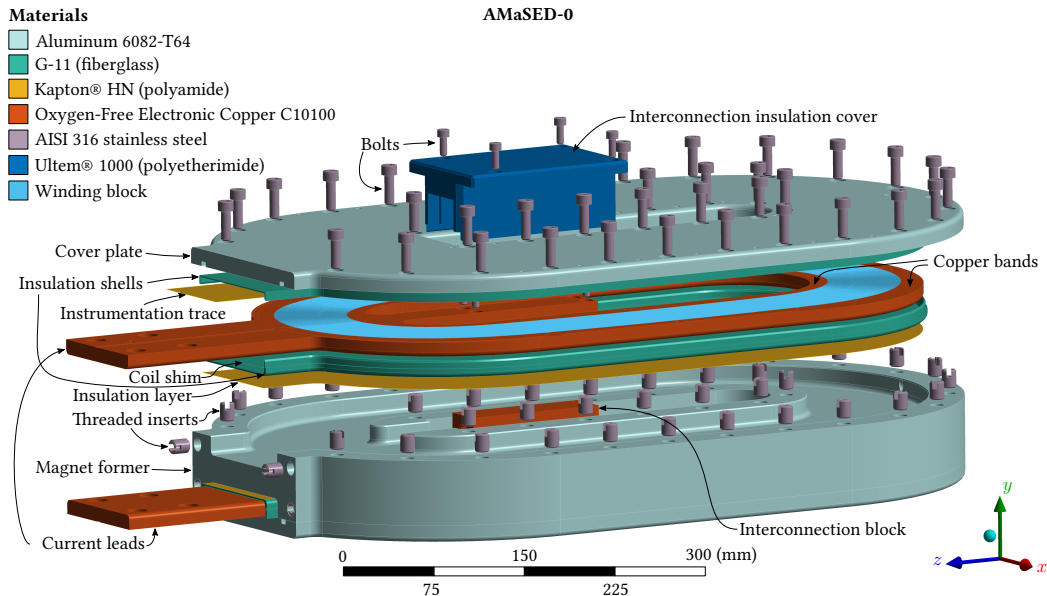


**Figure 12:** An exploded view of the components of the mechanical model coil, AMaSED-0.

## 4. Conclusion

We have presented ARCOS, a new concept for a magnetic spectrometer in space, capable to detect particles with rigidities up to 50 TV with a geometrical acceptance of  $2.8 \text{ m}^2\text{sr}$  for protons and antiprotons. The ARCOS magnet is a toroidal high-field HTS magnet providing a bending strength of 3 T m. We have presented the design of AMaSED-2 which is an HTS demonstrator coil for the ARCOS magnet. AMaSED-2 will be built in the CERN magnet laboratory.

## References

- [1] L. Rossi, M. Sorbi and P. Spillantini, *A superconducting magnetic lens for solar rays protection in manned interplanetary missions*, *IEEE Trans. Appl. Supercond.* **14** (2004) 1696.
- [2] F. Ambroglini, R. Battiston and W.J. Burger, *Evaluation of superconducting magnet shield configurations for long duration manned space missions*, *Front. Oncol.* **6** (2016) 97.
- [3] S. Ting, *The alpha magnetic spectrometer on the international space station*, *Nucl. Phys. B Proc. Suppl.* **243-244** (2013) 12.
- [4] M. Boezio, R. Munini and P. Picozza, *Cosmic ray detection in space*, *Prog. Part. Nucl. Phys.* **112** (2020) 103765.
- [5] L. Feng, R.-Z. Yang, H.-N. He, T.-K. Dong, Y.-Z. Fan and J. Chang, *AMS-02 positron excess: New bounds on dark matter models and hint for primary electron spectrum hardening*, *Phys. Lett. B* **728** (2014) 250.
- [6] AMS collaboration, *Antiproton flux, antiproton-to-proton flux ratio, and properties of elementary particle fluxes in primary cosmic rays measured with the alpha magnetic spectrometer on the international space station*, *Phys. Rev. Lett.* **117** (2016) 091103.
- [7] V. Poulin, P. Salati, I. Cholis, M. Kamionkowski and J. Silk, *Where do the AMS-02 antihelium events come from?*, *Phys. Rev. D* **99** (2019) 023016.
- [8] AMS collaboration, *Precision measurement of the proton flux in primary cosmic rays from rigidity 1 GV to 1.8 TV with the alpha magnetic spectrometer on the international space station*, *Phys. Rev. Lett.* **114** (2015) 171103.
- [9] S. Schael, A. Atanasyan, J. Berdugo, T. Bretz, M. Czupalla, B. Dachwald et al., *AMS-100: The next generation magnetic spectrometer in space – an international science platform for physics and astrophysics at lagrange point 2*, *Nucl. Instrum. Methods Phys. Res. A* **944** (2019) 162561.
- [10] R. Musenich, O. Adriani, B. Baudouy, V. Calvelli, S. Farinon, P. Papini et al., *A proposal for a superconducting space magnet for an antimatter spectrometer*, *IEEE Trans. Appl. Supercond.* **30** (2020) 1.
- [11] M. Dam, R. Battiston, W.J. Burger, R. Carpentiero, E. Chesta, R. Iuppa et al., *Conceptual design of a high temperature superconducting magnet for a particle physics experiment in space*, *Supercond. Sci. Technol.* **33** (2020) 044012.
- [12] H.-W. Kim, J. Hur, S.-W. Kim, S.-B. Kim, R.-K. Ko, D.-W. Ha et al., *Improvement in stability and operating characteristics of HTS coil using MIT material*, *IEEE Trans. Appl. Supercond.* **27** (2017) 1.
- [13] J. Mun, C. Lee, K. Sim, C. Lee, M. Park and S. Kim, *Electrical characteristics of soldered metal insulation REBCO coil*, *IEEE Trans. Appl. Supercond.* **30** (2020) 1.
- [14] K. Bouloukakis, M. Hunter, N. Long, R. Dykstra and B. Parkinson, *Discharge behaviour and modelling of a 1.5 T REBCO magnet with quench tolerant coils impregnated with conductive epoxy*, *IEEE Trans. Appl. Supercond.* **31** (2021) 1.
- [15] S. Agostinelli, J. Allison, K. Amako, J. Apostolakis, H. Araujo, P. Arce et al., *Geant4—a simulation toolkit*, *Nucl. Instrum. Methods Phys. Res. A* **506** (2003) 250.